Published in final edited form as:
J Biol Chem. 2000 December 8; 275(49): 38710–38715.

Store-operated Calcium Entry Inactivates at the Germinal Vesicle Breakdown Stage of *Xenopus* Meiosis*

Khaled Machaca‡ and **Shirley Haun**

From the Department of Physiology and Biophysics, University of Arkansas for Medical Sciences, Little Rock, Arkansas 72205

Abstract

Store-operated calcium entry (SOCE) is the predominant Ca^{2+} influx pathway in non-excitable cells and is activated in response to depletion of intracellular Ca^{2+} stores. We have studied SOCE regulation during *Xenopus* oocyte meiosis. SOCE can be measured readily in stage VI *Xenopus* oocytes arrested at the G_2–M transition of the cell cycle, either by Ca^{2+} imaging or by recording the SOCE current. However, following meiotic maturation, SOCE can no longer be activated by store depletion. We have characterized the time course of SOCE inactivation during oocyte maturation, and show that SOCE inactivates almost completely, in a very short time period, at the germinal vesicle breakdown stage of meiosis. This acute inactivation offers an opportunity to better understand SOCE regulation.

Ionic calcium (Ca^{2+}) is a universal second messenger important for many cellular responses ranging from gene expression to fertilization (1). Ca^{2+} signaling is mediated by a rise in cytoplasmic Ca^{2+}, either by Ca^{2+} release from intracellular stores or Ca^{2+} influx from the extracellular space. In non-excitable cells the primary Ca^{2+} influx pathway is store-operated calcium entry (SOCE)[1] (2). SOCE is activated in response to depletion of intracellular calcium stores and has been implicated in several cellular processes, including T-cell activation (3,4) and regulation of exocytosis (5–7). However the mechanism(s) coupling store depletion to SOCE activation remain unknown. The following three models have been proposed: “physical coupling,” “diffusible messenger,” and “vesicle fusion.” The physical coupling hypothesis proposes that SOCE channels couple directly to a Ca^{2+} sensor on the endoplasmic reticulum membrane, possibly the IP_3 receptor, in analogy to the dihydropyridineryanodine receptor interaction in skeletal muscle (8–10). Whereas the diffusible messenger hypothesis argues that store depletion results in the generation of a diffusible messenger that opens SOCE channels (11–13), the vesicle fusion model proposes that SOCE channels are inserted in the plasma membrane following store depletion (14). Although there is some evidence for each model (2), it is not yet clear what the coupling mechanism is and whether SOCE is activated by the same mechanism in different cell types.

Despite the importance and ubiquitous nature of Ca^{2+} signaling pathways, their role and regulation during the cell cycle remain controversial. Probably the clearest example of a Ca^{2+} requirement during the cell cycle is at fertilization, where a Ca^{2+} signal is necessary and sufficient for egg activation and the initiation of embryonic development (15,16). Oocytes of

*The costs of publication of this article were defrayed in part by the payment of page charges. This article must therefore be hereby marked “*advertisement*” in accordance with 18 U.S.C. Section 1734 solely to indicate this fact.

‡ To whom correspondence should be addressed. Tel.: 501-603-1596; Fax: 501-686-8167; E-mail: MachacaKhaledA@uams.edu..

[1]The abbreviations used are: SOCE, store-operated calcium entry; GVBD, germinal vesicle breakdown; I_{Cl1} and I_{Cl2} or $I_{Cl, Ca}$, calcium-activated chloride currents; MPF, maturation promoting factor; BAPTA, 1,2-bis(2-aminophenoxy)ethane-*N*,*N*,*N*′,*N*′-tetraacetic acid; IP_3, inositol 1,4,5-trisphosphate; CG, cortical granule; I_{SOCE}, SOCE current; I-V, current-voltage relationship; $GVBD_{50}$, the time from progesterone addition until 50% of the cells undergo GVBD.

both *Xenopus* and mammals are arrested at the G_2–M transition of the cell cycle (15,17). Before such oocytes become competent to be fertilized and able to support embryonic development, they undergo a maturation process called meiotic (or oocyte) maturation. During this maturation period oocytes enter meiosis, complete the first meiotic division with the extrusion of a polar body, and arrest at metaphase of the second meiotic division (metaphase II) (17). Cells remain arrested at metaphase II until fertilization, which relieves the metaphase II block and induces the completion of meiosis and entry into the mitotic cell cycle. In all animals studied, fertilization induces a rise in cytoplasmic Ca^{2+} levels that underlies most of the early events of egg activation (16). Henceforth, we will refer to immature stage VI *Xenopus* oocytes arrested at G_2–M as "oocytes" and cells after meiotic maturation (arrested at metaphase II) as "eggs."

In this report we show that SOCE becomes uncoupled from Ca^{2+} store content following meiotic maturation. In other words, store depletion in eggs does not activate SOCE. This shows that SOCE can be regulated independently of calcium load in the stores. We have further determined the time course of SOCE down-regulation during meiosis and show that SOCE inactivates acutely at the germinal vesicle breakdown (GVBD) stage.

EXPERIMENTAL PROCEDURES

Imaging and Electrophysiological Methods

Oocytes were isolated as described previously (20). Eggs were matured *in vitro* by incubation in 5 μg/ml progesterone. *Xenopus* oocytes or eggs were voltage clamped with two microelectrodes by the use of a GeneClamp 500 (Axon Instruments). Electrodes were filled with 3 M KCl and had resistances of 1–2 megohms. Voltage stimulation and data acquisition were controlled using either pClamp8 (Axon Instruments) or Curcap30 (developed by Bill Goolsby, Emory University). Confocal Ca^{2+} imaging was performed using an Olympus Fluoview confocal scanning system fitted to an IX70 microscope using a × 10 (0.3 numerical aperature) objective. Images (256 × 256 pixels) were collected and analyzed using Olympus Fluoview software.

Oocyte capacitance was measured by administering 4 consecutive voltage steps from a −40-mV holding potential to −30 mV for 50 ms each. Capacitive current decay was averaged and fitted by a single exponential. Membrane capacitance (C_m) was calculated as follows: $C_m = \tau (1/R_a + G_m)$. τ is the time constant obtained from the exponential fit. R_a is the access resistance and was calculated as follows: $R_a = V_p/I_0$. V_p is the applied voltage pulse (10 mV), and I_0 is the instantaneous current obtained by extrapolating the experimental fit to time 0. G_m was calculated as follows : $G_m = I_{ss}/(V_p - R_a*I_{ss})$. I_{ss} is the steady state current following relaxation of the capacitive transient (18,19).

Immunohistochemistry

Cells were fixed in 100% methanol and incubated overnight at −20 °C. Oocytes were bisected in half and incubated in 1:250 dilution of DM1A, an anti-tubulin monoclonal antibody (Sigma) in Tris-buffered saline containing 2% bovine serum albumin for 16 h. After several washes cells were incubated in 1:100 dilution of a fluorescein isothiocyanate-labeled goat anti-mouse secondary antibody (Sigma) for 16 h. Oocytes were washed, dehydrated, stained in 5 μg/ml propidium iodide, and cleared in benzyl alcohol:benzyl benzoate (1:2) before confocal imaging.

MPF Kinase Assay

MPF kinase activity was measured by lysing 5 oocytes in 100 μl of extraction buffer (80 mM β-glycerophosphate, 20 mM Hepes, pH 7.5, 20 mM EGTA, 15 mM $MgCl_2$, 1 mM sodium

vanadate, 50 mM sodium fluoride, 1 mM dithiothreitol, 10 μg/ml aprotinin, 50 μg/ml leupeptin, 1 mM phenylmethylsulfonyl fluoride). Lysates were centrifuged at 16,000 × *g* for 5 min, and the supernatant was stored at −70 °C until use in the kinase assay. The H1 kinase assay to measure MPF activity was performed using the SignaTECT™kinase kit (Promega).

RESULTS

We have studied the regulation of SOCE during *Xenopus* oocyte meiotic maturation. As in most non-excitable cells, depletion of intracellular Ca^{2+} stores in *Xenopus* oocytes activates SOCE. We have recently developed a protocol to image SOCE in *Xenopus* oocytes (20) (Fig. 1). Ca^{2+} release and SOCE are temporally separated by recording Ca^{2+} levels using confocal imaging in voltage-clamped cells stepped sequentially to +40 and −140 mV (Fig. 1*A*). Ca^{2+} release from stores is independent of plasma membrane voltage and occurs at both +40 and −140 mV, whereas Ca^{2+} influx occurs only at −140 mV because of the larger driving force (20). Fig. 1*A* shows representative three-dimensional rendition images of Ca^{2+} release and SOCE in oocytes. Ca^{2+} release was triggered by IP_3 injection (2 pmol), which induces a sweeping wave of Ca^{2+} release. Initially, Ca^{2+} release is observed at the site of IP_3 injection (Fig. 1*A*, *i*) and slowly spreads through the entire cytoplasm (Fig. 1*A*, *ii*). Following store depletion SOCE becomes apparent as Ca^{2+} influx at −140 mV (Fig. 1*A*, *iii*). The time course of development of Ca^{2+} fluorescence over the confocal section at +40 (*squares*) and −140mV (*circles*) is shown in Fig. 1*B*. IP_3 injection induces Ca^{2+} release from stores and a steep increase in Ca^{2+} fluorescence at both voltages, followed by a slow decay to baseline. During the decay phase, Ca^{2+} fluorescence becomes gradually higher at −140 (*circles*) than at +40mV (*squares*) (Fig. 1*B*). The difference in Ca^{2+} fluorescence between images at −140 and +40 mV provides a measure of the extent of Ca^{2+} entry in response to store depletion, thus SOCE (Fig. 1*D*, *blue triangles*).

To study SOCE in eggs, we induced meiotic maturation with progesterone (5 μg/ml) and imaged SOCE as described above. Interestingly, store depletion does not activate SOCE in eggs (Fig. 1*C* and *D*). IP_3 injection induces Ca^{2+} release from stores, but in contrast to oocytes (Fig. 1*B*), no Ca^{2+} influx is observed at −140 mV (*circles*) up to 30 min after IP_3 injection (Fig. 1*C* and *D*). Furthermore, the dynamics of Ca^{2+} release were significantly different following oocyte maturation. Injection of IP_3 in eggs results in a slower and more prolonged Ca^{2+} release wave. Ca^{2+} release is defined as the time from the initial observation of the Ca^{2+} wave in the focal plane until peak Ca^{2+} fluorescence. This time was significantly shorter ($p < 0.00012$) in oocytes (36.67 ± 12.01 s; $n = 3$) *versus* eggs (167.5 ± 11.29 s; $n = 8$). An example of the time required to reach maximum Ca^{2+} fluorescence for an oocyte (*blue trace*) and an egg (*red trace*) is shown in the *inset* of Fig. 1*C*. In addition, half-time of decay of cytoplasmic Ca^{2+} levels, from peak Ca^{2+} fluorescence to half-maximal value, was significantly slower ($p < 0.037$) in eggs (305 ± 58.88 s; $n = 8$) (Fig. 1*C*) as compared with oocytes (60 ± 11.54 s; $n = 3$) (Fig. 1*B*).

Fig. 1*D* shows a summary of SOCE activation in oocytes and eggs from the same donor female. Whereas oocytes exhibit a robust SOCE signal ($t_{1/2}$= 4.3 min; see Fig. 1*D*, *blue triangles*), no SOCE activity is detected in eggs up to 20 min after Ca^{2+} release (Fig. 1*D*, *green triangles*). These data suggest that the coupling between store Ca^{2+} load and SOCE activation is somehow disrupted during oocyte maturation. This could be due to either the inactivation of SOCE channels or the inhibition of the coupling mechanism between store depletion and SOCE.

Ca^{2+} release in eggs results in cortical granule (CG) exocytosis, which releases several enzymes that modify proteins on the egg surface and induces the slow block to polyspermy (21). SOCE channels could be a target for these enzymes, which would explain SOCE inactivation in eggs. To test this possibility, we injected eggs with the Ca^{2+} chelator BAPTA to inhibit a rise in

cytoplasmic Ca^{2+} following store depletion. We confirmed that BAPTA injection inhibits CG exocytosis by assessing the appearance of the fertilization envelope (Fig. 2). *Xenopus* eggs are surrounded by a vitelline envelope that is in tight proximity with the cell membrane. Release of CG content creates a space between the vitelline and cell membranes called the fertilization envelope (21) (Fig. 2). Egg activation with the Ca^{2+} ionophore ionomycin (10 μ_M) results in Ca^{2+} release and the elevation of the fertilization envelope within ~2 min (Fig. 2). In contrast, no fertilization envelope was detected in BAPTA-injected eggs as long as 15 min after egg activation with ionomycin (Fig. 2). This shows that BAPTA was effective in buffering cytoplasmic Ca^{2+} and inhibiting CG fusion.

To assess whether SOCE can be detected when CG fusion is inhibited, we were interested in measuring SOCE in BAPTA-injected eggs. Because BAPTA injection precludes measuring SOCE by imaging, we recorded the SOCE current (I_{soce}) directly as described by Yao and Tsien (22). Stage VI *Xenopus* oocytes exhibited a prominent SOCE current in response to store depletion (Fig. 3). I_{soce} was measured using a ramp voltage from −140 to +60 mV applied to oocytes preinjected with BAPTA once every 30 s (Fig. 3*A*). We depleted Ca^{2+} stores by IP_3 injection and followed the development of SOCE by monitoring the inward current at − 140 mV (Fig. 3*B*). As described previously (22), I_{soce} was measured as the La^{3+}-inhibited current induced in response to store depletion (Fig. 3, *B–D*). The I_{soce} current-voltage relationship (I-V) had the typical inward rectifying character (Fig. 3*D*), as described by others (2,22). We further determined the I-V of the SOCE current using a step voltage protocol, which resulted in a similar inward rectifying curve (data not shown).

When we attempted to record I_{soce} from *Xenopus* eggs preinjected with BAPTA using the same protocol outlined above, in agreement with our imaging data, no SOCE current could be detected following depletion of Ca^{2+} stores with either ionomycin or IP_3 (Fig. 4, *A–C*). In contrast Ca^{2+} store depletion in oocytes from the same donor female induced a prominent I_{soce} (Fig. 4, *A–C*). This shows that SOCE inactivates specifically during *Xenopus* oocyte meiosis, independently of CG fusion.

To determine whether other membrane currents are down-regulated in eggs, we measured the activity of Ca-activated chloride currents ($I_{Cl,\ Ca}$) following meiotic maturation (Fig. 4, *D–F*). Hartzell (23) described two $I_{Cl,\ Ca}$ in *Xenopus* oocytes, I_{Cl1} and I_{Cl2}. I_{Cl1} responds to Ca^{2+} release from stores, whereas I_{Cl2} responds only to Ca^{2+} influx from the extracellular space but not Ca^{2+} release. I_{Cl1} has an outward rectifying I-V and is therefore activated at depolarizing voltages (+40 mV). In contrast I_{Cl2} exhibits an inward rectifying I-V and is measured at hyperpolarizing voltages (−140 mV) (Fig. 4*D*). We measured the development of I_{Cl1} and I_{Cl2} in oocytes and eggs voltage clamped using the protocol shown in Fig. 4*D*. In oocytes, I_{Cl1} activates following IP_3 injection in response to Ca^{2+} release from stores (20) (Fig. 4*D*, *squares*). As Ca^{2+} stores become depleted I_{Cl1} returns to baseline. Ca^{2+} influx through SOCE channels following store depletion slowly activates I_{Cl2} (20) (Fig. 4*D*, *circles*).

The activation of the calcium-activated chloride currents in response to IP_3 injection was very different in eggs (Fig. 4*E*). As expected from SOCE inactivation in eggs, I_{Cl2} was not activated following store depletion (Fig. 4*E*, *circles*), whereas I_{Cl1} activated in response to Ca^{2+} release was significantly larger and more prolonged in eggs (Fig. 4*E*, *squares*). These changes in the I_{Cl1} response are most likely due to the altered Ca^{2+} release dynamics in eggs (see Fig. 1*C*). Nonetheless, these data show that I_{Cl1} is not down-regulated during meiotic maturation.

$I_{Cl,\ Ca}$ is required for the fast electrical block to polyspermy at fertilization (24). It is therefore critical that this current remains active in eggs. The inactivation of SOCE, but not $I_{Cl,\ Ca}$, shows that oocytes differentially regulate membrane currents during maturation to generate developmentally competent eggs.

Oocyte maturation in *Xenopus* induces a gradual decrease in plasma membrane surface area (see Fig. 6*A*), which is responsible for the down-regulation of plasma membrane Na^+-K^+-ATPase (25,26). To determine whether SOCE channels are subject to the same regulation, we correlated I_{soce} levels with the different phases of meiosis (see Figs. 5 and 6). We followed the progression of meiosis by tracking the nuclear cycle after progesterone addition. Oocytes were stained for tubulin (anti-tubulin antibody) and DNA (propidium iodide) (Fig. 5*a*). From the time of progesterone addition until GVBD, the nuclear envelope is intact with no DNA condensation (Fig. 5*a*, *A*). GVBD is easily monitored by the appearance of a white spot on the animal hemisphere (17). White spot appearance correlated nicely with actual GVBD in experiments similar to the one represented by Fig. 5*a* (data not shown). At GVBD, the chromosomes are readily apparent, but they are still spread over a relatively large area, and the spindle is not formed (Fig. 5*a*, *B*). During the 2.5–3 h following GVBD, oocytes complete meiosis I (Fig. 5*a*, *C–F*), enter meiosis II, and arrest at metaphase II (Fig. 5*a*, *G–I*).

It is also possible to follow the progression of meiosis by measuring MPF kinase activity, which cycles during meiosis with peak activity at metaphase (17). We measured $p34^{cdc2}$ kinase activity during oocyte maturation from the same batch of cells on which we performed immunofluorescence (Fig. 5*b*). MPF activity is maximal at GVBD and decreases between meiosis I and meiosis II before peaking again at metaphase II (Fig. 5*b*).

To determine the time course of SOCE inactivation during meiotic maturation, we recorded I_{soce} at different time points during the maturation process, from the same batch of cells on which we performed immunofluorescence and measured MPF activity. The experiment was repeated three times with cells from different females. The time from progesterone addition until GVBD varied between different batches of cells. We therefore normalized the data such that one time unit is defined as the time from progesterone addition until 50% of the cells undergo GVBD ($GVBD_{50}$) (27). We recorded both I_{soce} (Fig. 6*B*) and membrane capacitance (Fig. 6*A*) to obtain a measure of membrane surface area and I_{soce} density (Fig. 6*C*). This analysis resulted in the dramatic finding that SOCE inactivates over a very narrow time period (<15 min) right at GVBD. I_{soce} was always present in every cell we recorded from before GVBD (n = 21), at similar levels to I_{soce} in oocytes (Fig. 6*B*, *Early* and *Late No GVBD*). We recorded from cells after progesterone addition as early as 0.21 up to 1.3 $GVBD_{50}$, with no decrease in I_{soce} levels. During that time membrane capacitance decreases by ~20% (Fig. 6*A*), resulting in higher I_{soce} density in the cells that are delayed in undergoing GVBD (*Late No GVBD*) (Fig. 6*C*). However, as soon as GVBD occurs, I_{soce} is no longer detectable (Fig. 6*B*, *GVBD*). Cells were checked for GVBD every 5 min, and we recorded I_{soce} ~5 min after GVBD. Therefore within approximately 15 min I_{soce} inactivates almost completely (Fig. 6*B*). This is quite remarkable considering that meiotic maturation, from progesterone addition until metaphase II, requires 7–12 h depending on the batch of oocytes.

After GVBD, I_{soce} remains inactivated throughout oocyte maturation until metaphase II. We measured I_{soce} at 0.5, 1, 1.5, 2, 3, 4, and 5 h after GVBD (n = 24) and never observed any I_{soce} activity. These data show that I_{soce} inactivates at GVBD and remains inactivated through the completion of oocyte maturation.

DISCUSSION

It is unlikely that SOCE inactivation is due to membrane internalization during meiotic maturation, because there is no correlation between membrane area (Fig. 6*A*) and SOCE levels (Fig. 6*B*). Whereas membrane area decreases gradually after progesterone addition, SOCE inactivates acutely at GVBD. The Na^+-K^+-ATPase has also been shown to be down-regulated during meiotic maturation because of sequestration into intra-cellular vesicles (25,26). In this case Na^+-K^+-ATPase activity begins to decrease gradually after progesterone addition, even

before GVBD, and continues after GVBD has occurred (28). Furthermore complete down-regulation of the Na^+-K^+-ATPase requires almost 2 h (28). This is in sharp contrast to the rapid and complete inactivation of SOCE at GVBD (Fig. 6*B*).

MPF activity is maximal at GVBD (Fig. 5*b*). It is therefore tempting to propose that MPF plays a role in SOCE inactivation. However, SOCE current does not cycle in tandem with MPF activity during the later stages of meiosis (see Figs. 5*b* and 6*B*). Whereas MPF kinase activity declines between meiosis I and II, SOCE remains undetectable throughout this transition (Fig. 6*B*). Although this does not rule out a direct role for MPF in the initial inactivation of SOCE, it suggests that other mechanism(s) are involved in maintaining SOCE inactivation.

The regulation of membrane proteins during the cell cycle is not unique to SOCE. Several currents have been shown to be cell cycle-dependent. In mouse embryos K^+ currents are present during M and G_1 but not S and G_2 (30), and in ascidian embryos an inward rectifying Cl^- current has been shown to fluctuate with the cell cycle (31). In addition, cell cycle regulation of exogenously expressed channel proteins in *Xenopus* oocytes has been reported. The rat ether-a-go-go K^+ channel alters its voltage dependence during meiotic maturation through an MPF-mediated process (32). However, to our knowledge, none of these currents exhibit a similar regulation to the rapid and complete inactivation observed for SOCE. This argues that SOCE inactivation is regulated by distinct mechanisms. Furthermore, SOCE might be down-regulated during mitosis in mammalian cells (29), arguing that SOCE inactivation could potentially be a universal phenomenon during M phase.

Although at this point we do not know the mechanism controlling SOCE inactivation, anyone of the aforementioned coupling mechanisms could be disrupted during meiosis leading to SOCE inactivation. However, because vesicle trafficking is down-regulated during mitosis (33), we favor the idea that SOCE inactivation during oocyte maturation is because of disruption of vesicle fusion.

Acknowledgements

We thank Lou DeFelice, Richard Kurten, and Mike Jennings for comments on the manuscript and Criss Hartzell for continued support.

References

1. Berridge MJ. Bioessays 1995;17:491–500. [PubMed: 7575490]
2. Parekh AB, Penner R. Physiol Rev 1997;77:901–930. [PubMed: 9354808]
3. Serafini A, Lewis RS, Clipstone NA, Bram R, Fanger C, Fiering S, Herzenberg LA, Crabtree GR. Immunity 1995;3:239–250. [PubMed: 7648396]
4. Fanger C, Hoth M, Crabtree GR, Lewis RS. J Cell Biol 1995;131:655–667. [PubMed: 7593187]
5. Fomina AF, Nowycky MC. J Neurosci 1999;19:3711–3722. [PubMed: 10234003]
6. Koizumi S, Inoue K. Biochem Biophys Res Commun 1998;247:293–298. [PubMed: 9679028]
7. Dolmetsch RE, Lewis RS. J Gen Physiol 1994;103:365–388. [PubMed: 8195779]
8. Berridge MJ. Biochem J 1995;312:1–11. [PubMed: 7492298]
9. Irvine RF. FEBS Lett 1990;263:5–9. [PubMed: 2185036]
10. Rosado JA, Jenner S, Sage SO. J Biol Chem 2000;275:7527–7533. [PubMed: 10713057]
11. Randriamampita C, Tsien RY. Nature 1993;364:809–814. [PubMed: 8355806]
12. Gilon P, Bird GS, Bian X, Yakel JL, Putney JW Jr. J Biol Chem 1995;270:8050–8055. [PubMed: 7713906]
13. Csutora P, Su Z, Kim HY, Bugrim A, Cunningham KW, Nuccitelli R, Keizer JE, Hanley MR, Blalock JE, Marchase RB. Proc Natl Acad Sci U S A 1999;96:121–126. [PubMed: 9874782]
14. Somasundaram B, Norman JC, Mahaut-Smith MP. Biochem J 1995;309:725–729. [PubMed: 7639685]

15. Miyazaki S. CIBA Found Symp 1995;188:235–251. [PubMed: 7587620]
16. Stricker SA. Dev Biol 2000;211:157–176. [PubMed: 10395780]
17. Smith LD. Development 1989;107:685–699. [PubMed: 2698799]
18. Takahashi A, Watkins SC, Howard M, Frizzell RA. Am J Physiol 1996;271:C1887–C1894. [PubMed: 8997189]
19. Neher E, Marty A. Proc Natl Acad Sci U S A 1982;79:6712–6716. [PubMed: 6959149]
20. Machaca K, Hartzell HC. J Gen Physiol 1999;113:249–266. [PubMed: 9925823]
21. Grey RD, Wolf DP, Hedrick JL. Dev Biol 1974;36:44–61. [PubMed: 4822839]
22. Yao Y, Tsien RY. J Gen Physiol 1997;109:703–715. [PubMed: 9222897]
23. Hartzell HC. J Gen Physiol 1996;108:157–175. [PubMed: 8882861]
24. Grey RD, Bastiani MJ, Webb DJ, Schertel ER. Dev Biol 1982;89:475–484. [PubMed: 7056442]
25. Schmalzing G, Eckard P, Kroner S, Passow H. Am J Physiol 1990;258:C179–C184. [PubMed: 2154110]
26. Vasilets LA, Schmalzing G, Madefessel K, Haase W, Schwarz W. J Membr Biol 1990;118:131–142. [PubMed: 2176238]
27. Wasserman WJ, Masui Y. Exp Cell Res 1975;91:381–388. [PubMed: 165088]
28. Richter HP, Jung D, Passow H. J Membr Biol 1984;79:203–210. [PubMed: 6088774]
29. Preston SF, Sha'afi RI, Berlin RD. Cell Regul 1991;2:915–925. [PubMed: 1809398]
30. Day ML, Pickering SJ, Johnson MH, Cook DI. Nature 1993;365:560–562. [PubMed: 8413614]
31. Coombs JL, Villaz M, Moody WJ. Dev Biol 1992;153:272–282. [PubMed: 1397684]
32. Pardo LA, Bruggemann A, Camacho J, Stuhmer W. J Cell Biol 1998;143:767–775. [PubMed: 9813096]
33. Warren G. Annu Rev Biochem 1993;62:323–348. [PubMed: 8352593]

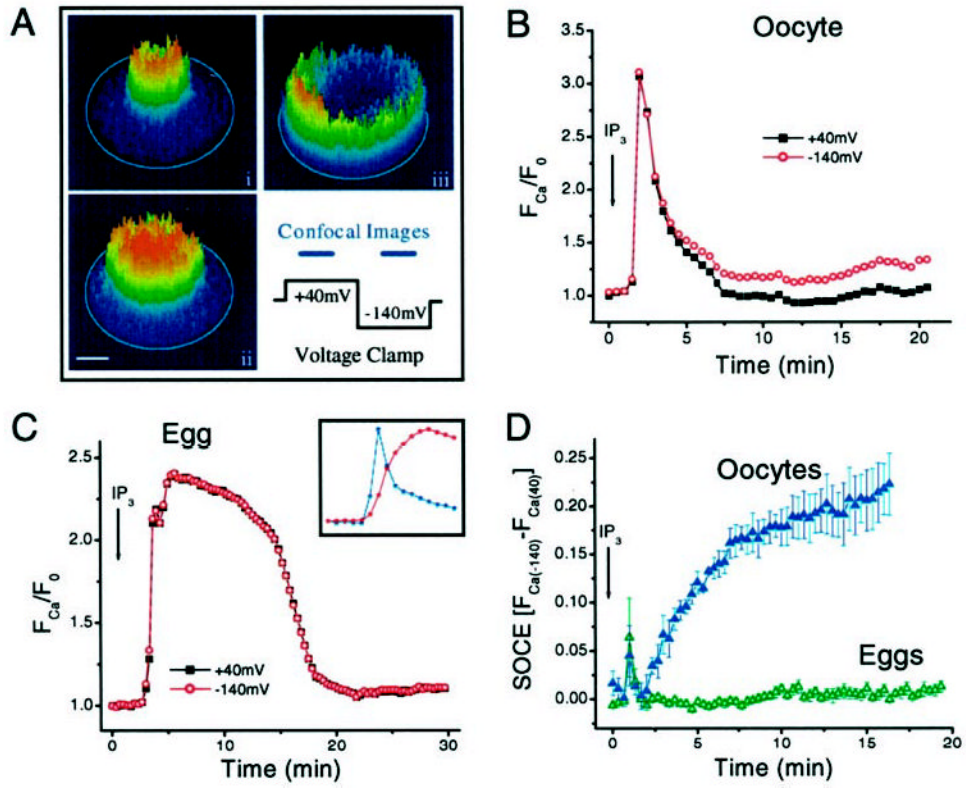

Fig. 1. Imaging SOCE.

Albino oocytes were loaded with Ca-green-1 coupled to 70-kD dextran (7 μm) and voltage clamped from a holding potential of 0 to +40 then −140 mV for 1 s each as shown in *A*. Confocal images were collected 300 msec into each voltage pulse. *A*, representative three-dimensional images of Ca^{2+} release at +40 mV (*I* and *ii*) and Ca^{2+} influx at −140 mV (*iii*). Although the images in *panels i* and *ii* were taken at +40 mV, identical images were obtained in the following −140-mV voltage pulse: *panels i*, *ii*, and *iii* were taken 10 s, 2 min, and 10 min, respectively, after IP_3 injection. *Scale bar* is 150 μm. *B* and *C*, Ca^{2+} fluorescence (F_{Ca}) over time at +40 and −140 mV from an oocyte (*B*) and an egg (*C*). The *inset* in *C* shows superimposed traces of Ca^{2+} fluorescence on an expanded scale from an oocyte (*blue trace*) and an egg (*red trace*). This illustrates the slower Ca^{2+} release kinetics in eggs. *D*, SOCE in eggs (n = 10) and oocytes (n = 3). SOCE was calculated as the difference between F_{Ca} at −140 and + 40 mV. Eggs were matured in 5 μg/ml progesterone. The external solution was 123 mm NaCl, 2.5 mm KCl, 2 mm $CaCl_2$, 2 mm $MgCl_2$, 10 mM Hepes, pH 7.4.

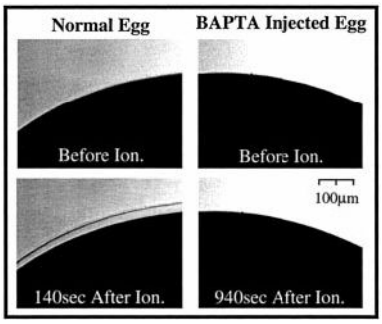

Fig. 2. BAPTA inhibits cortical granule fusion.

Egg activation with ionomycin (10 μm) results in the elevation of the fertilization envelope because of cortical granule fusion in eggs (*left panels*, $n = 3$). In contrast no fertilization envelope can be detected in eggs preinjected with 7 nmol of BAPTA (*right panels*, $n = 4$).

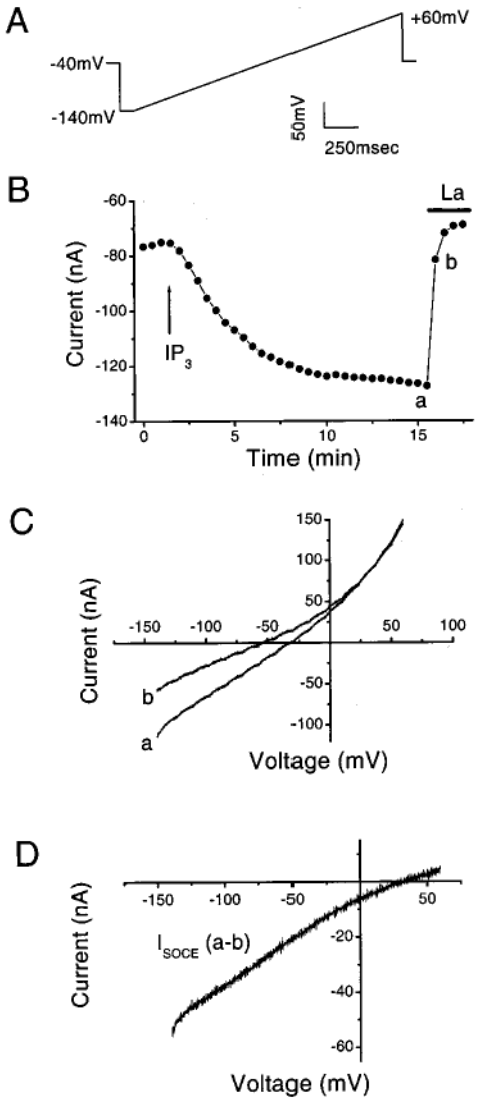

Fig. 3. Recording I_{soce} from oocytes.

Cells were injected with 7 nmol of BAPTA and voltage clamped using the ramp shown in *A* once every 30 s. *B*, stores were depleted by IP_3 injection (2 pmol), which induced an inward current at −140 mV, the time course of which is shown. To measure I_{soce}, 0.1 mM La^{3+} (*La*) was added at the end of the experiment. The external solution was 30 mm $CaCl_2$, 55 mm NaCl, 10 mM Hepes, pH 7.2. *C*, I_{soce} was measured as the La^{3+}-inhibited current after store depletion. Current ramps before (*a*) and after (*b*) La^{3+} addition are shown. *D*, I_{soce} current-voltage relationship was obtained as the difference between the currents before and after La^{3+} addition.

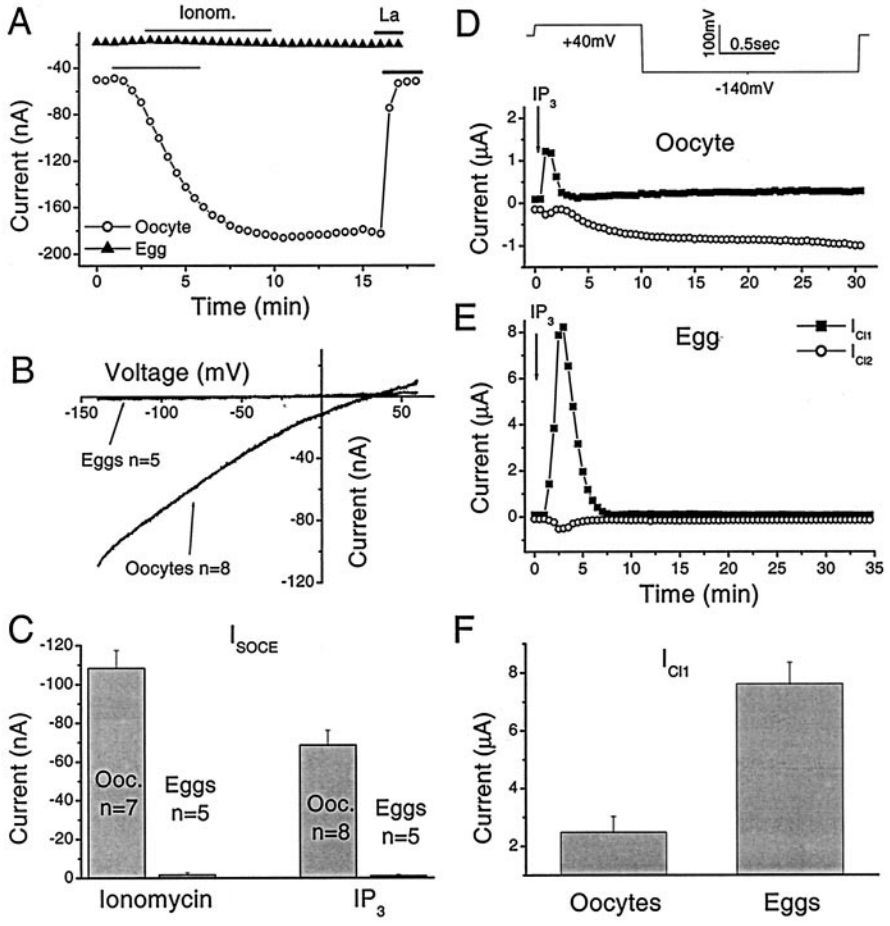

Fig. 4. I_{soce} is inactivated in eggs.

A, the same protocol outlined in the legend of Fig. 2 was used to record I_{soce}. Time course of I_{soce} activation in oocytes (*circles*) and eggs (*triangles*) in response to ionomycin (10 μm) is shown. The *bars above* the *traces* indicate ionomycin (*Ionom.*) and La^{3+} (*La*) addition (0.1 mm). Data show the current at −140 mV. *B*, current-voltage relationship of I_{soce} in oocytes and eggs. *C*, average I_{soce} at −140 mV in oocytes and eggs following store depletion with ionomycin or IP_3. The *number* of cells per treatment is indicated. $I_{Cl, Ca}$ in oocytes and eggs is as follows: cells were voltage clamped using the protocol shown in *D*. IP_3 injection (2 pmol) is indicated by the *arrow*. *D* and *E*, time course of $I_{Cl, Ca}$ development. I_{Cl1} (*squares*) was measured as the maximal current at +40 mV, and I_{Cl2} was measured as the maximal current at −140 mV as described previously (20). *F*, I_{Cl1} was significantly larger ($p < 0.00052$) in eggs as compared with oocytes ($n = 5$).

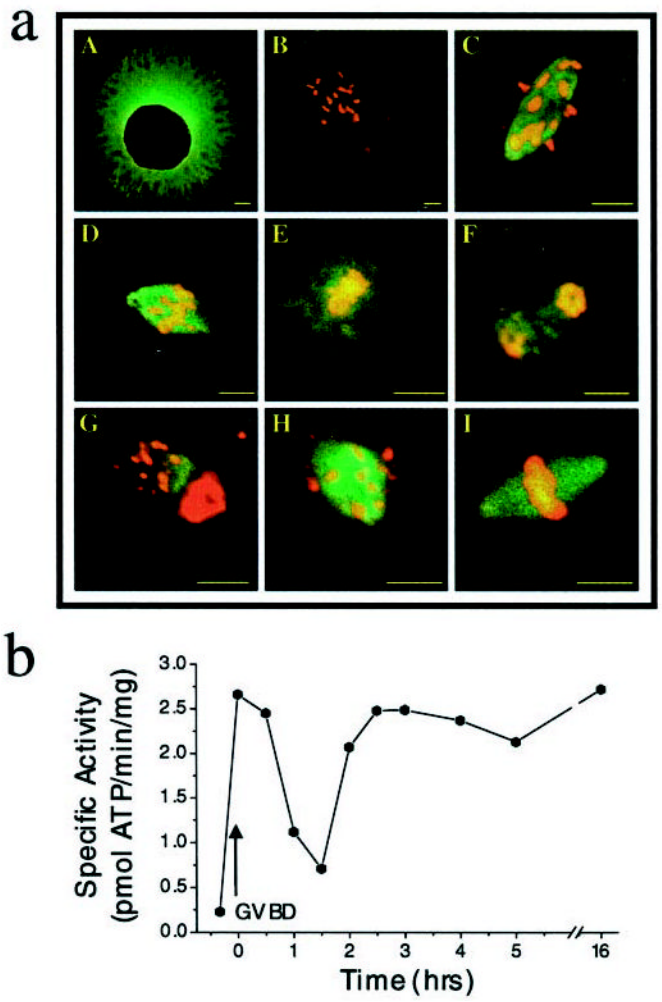

Fig. 5. Stages of meiosis.

a, oocytes were fixed at different time points after progesterone addition and stained with propidium iodide to visualize the chromosomes and an anti-tubulin antibody to visualize the structure of the spindle. *A*, germinal vesicle intact oocytes, before GVBD. *B*, GVBD as indicated by a *white spot* on the animal hemisphere. *C*, prometaphase I, 30 min after GVBD. *D*, metaphase I, 1–1.5 h after GVBD. *E*, anaphase I, 2–2.5 h after GVBD. *F*, telophase I, 2–2.5 h after GVBD. *G*, end of prophase II, 2.5–3 h after GVBD. Note the *diffuse staining* of the DNA in the *polar body*. *H*, prometaphase II, 2.5–3 h after GVBD. *I*, metaphase II, 3–16 h after GVBD. The *scale bars* in all the *panels* are 10 μm, except for *panel A*, where it is 100 μm. *b*, MPF kinase activity during meiotic maturation. *Time 0* refers to GVBD as indicated by the *arrow*.

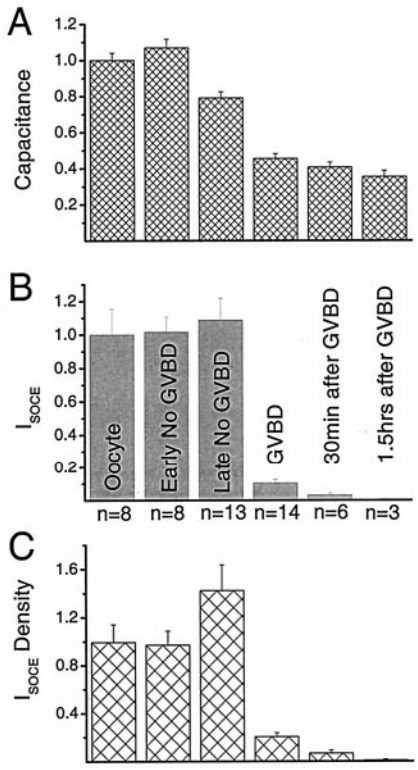

Fig. 6. SOCE inactivates at GVBD.

I_{soce} (*A*) and cell capacitance (*B*) were measured at different time points after progesterone addition. *C*, I_{soce} density obtained as the current density per unit area (I_{soce}/capacitance). The data was normalized to values in oocytes because of the variability observed between cells from different donor females. *Labeling* in *B* applies to *A* and *C*. *Early No GVBD* refers to cells that have been in progesterone for less than $GVBD_{50}$, and *Late No GVBD* refers to cells that have been in progesterone from more than $GVBD_{50}$ up to 1.3 $GVBD_{50}$. We measured I_{soce} in eggs at 0.5, 1, 1.5, 2, 3, 4, and 5 h after GVBD, and no SOCE current could be detected. Data for the 0.5- and 1.5-h time points are shown. The *number* of cells at each time point is indicated.